Computational Study on the Kinetics and Mechanisms for the Unimolecular Decomposition of Formic and Oxalic Acids†

Jee-Gong Chang,*,‡,§ Hsin-Tsung Chen,*,§ Shucheng Xu,§ and M. C. Lin§,||

National Center for High-performance Computing, Taiwan, Department of Chemistry, Emory University, Atlanta, Georgia 30322, Center for Interdisciplinary Molecular Science, National Chiao Tung University, Hsichu, Taiwan 300

Received: December 29, 2006; In Final Form: February 6, 2007

The kinetics and mechanisms for the unimolecular decomposition reactions of formic acid and oxalic acid have been studied computationally by the high-level G2M(CC1) method and microcanonical RRKM theory. There are two reaction pathways in the decomposition of formic acid: The dehydration process starting from the *Z* conformer is found to be the dominant, whereas the decarboxylation reaction starting from the *E* conformer is less competitive. The predicted rate constants for the dehydration and decarboxylation reactions are in good agreement with the experimental data. The calculated CO/CO_2 ratio, 13.6−13.9 between 1300 and 2000 K, is in close agreement with the ratio of 10 measured experimentally by Hsu et al. (In *The 19th International Symposium on Combustion*; The Combustion Institute: Pittsburgh, PA, 1983; p 89). For oxalic acid, its isomer with two intramolecular hydrogen bonds is the most stable structure, similar to earlier reports. Two primary decomposition channels of oxalic acid producing CO_2 + HOCOH with barriers of 33−36 kcal/mol and $CO_2 + CO + H_2O$ with a barrier of 39 kcal/mol were found. At high temperatures, the latter process becomes more competitive. The rate constant predicted for the formation of CO_2 and HOCOH (the precursor of HCOOH) agrees well with available experimental data. The mechanism for the isomerization of HOCOH to HCOOH is also discussed.

Introduction

Carboxylic acids such as formic acid and oxalic acid are key intermediates in the oxidation of organic hydrocarbons in atmospheric chemistry.[1] The unimolecular decomposition of formic acid is well-known to take place by the dehydration and decarboxylation pathways

$$HCOOH \rightarrow H_2O + CO \quad (1)$$

$$\rightarrow CO_2 + H_2 \quad (2)$$

Many studies on the unimolecular decomposition of formic acid in the gas phase, both experimental[2−5] and theoretical,[6−10] have been reported. The experiments show that CO production is much greater than CO_2 production, indicating that dehydration is the main pathway. The measured activation energies (E_a)[2−5] of dehydration and decarboxylation vary in wide ranges: 32−66 and 48−68 kcal/mol, respectively. Theoretically, earlier studies[2,4,8,9,11] using low-level ab initio molecular orbital (MO) calculations predicted the barrier of decarboxylation to be 20−30 kcal/mol higher than that of dehydration, whereas recent studies[6,7,9,10,12] using high-level methods obtained barrier differences of only a few kilocalories per mole between the two pathways. Only the theoretical data obtained by the high-level calculations are close to the highest E_a values of experiments mentioned above. To date, the question of the CO/CO_2 product branching ratio of 10 reported by Hsu et al.[3] remains unexplained and difficult to predict if the barrier (threshold) energies of the two channels are almost the same. It is thus necessary to use high-level ab initio and reaction theory calculations to resolve this issue.

Similarly, the thermal decomposition of oxalic acid has been investigated in many experimental[13−18] and theoretical[19−21] studies. Lapidus et al.[15] found that equimolar quantities of CO_2 and HCOOH were the main products in the temperature range 400−430 K with the Arrhenius parameters $E_a = 30.0 \pm 1.3$ kcal/mol and $\log(A/s^{-1}) = 11.9 \pm 0.7$. Yamamoto and Back[18] studied the photolysis of oxalic acid at 257−313 nm. Two primary decomposition channels producing CO_2 + HCOOH and $CO_2 + CO + H_2O$ were found. The formation of the former products was found to be at least 2.6 times faster than the formation of the latter. In contrast, Kakumoto et al.[14] predicted that $CO_2 + CO + H_2O$ should be the major products; they estimated the barrier for the formation of CO_2 + HCOOH to be about 35 kcal/mol higher by an ab initio study at the MP2/4-31G//HF/3-21G level. To interpret the disparity between the experimental and theoretical results, Bock and Redington[19] suggested that a bimolecular process for the isomerization of the dihydroxycarbene formed in the decomposition to formic acid via proton exchange might occur by a collisional complex and facilitate the production of HCOOH. Higgins et al.[20] examined this proposal using H_2O as a catalyst at the MP4SDQ/6-311++G(d,p)//B3LYP/6-31G(d) level. Their results indicated that this bimolecular channel might be significant for the rapid formation of CO_2 + HCOOH.

As presented above, many investigations on the decomposition reactions of formic acid and oxalic acid in the gas phase have been performed. However, there have been no quantitative

† Part of the special issue "M. C. Lin Festschrift".

* To whom correspondence should be addressed. E-mail: changjg@nchc.org.tw (J.-G.C.), hchen9@emory.edu (H.-T.C.).

‡ National Center for High-performance Computing.

§ Emory University.

|| National Chiao Tung University.

10.1021/jp069036p CCC: $37.00
Published on Web 03/06/2007

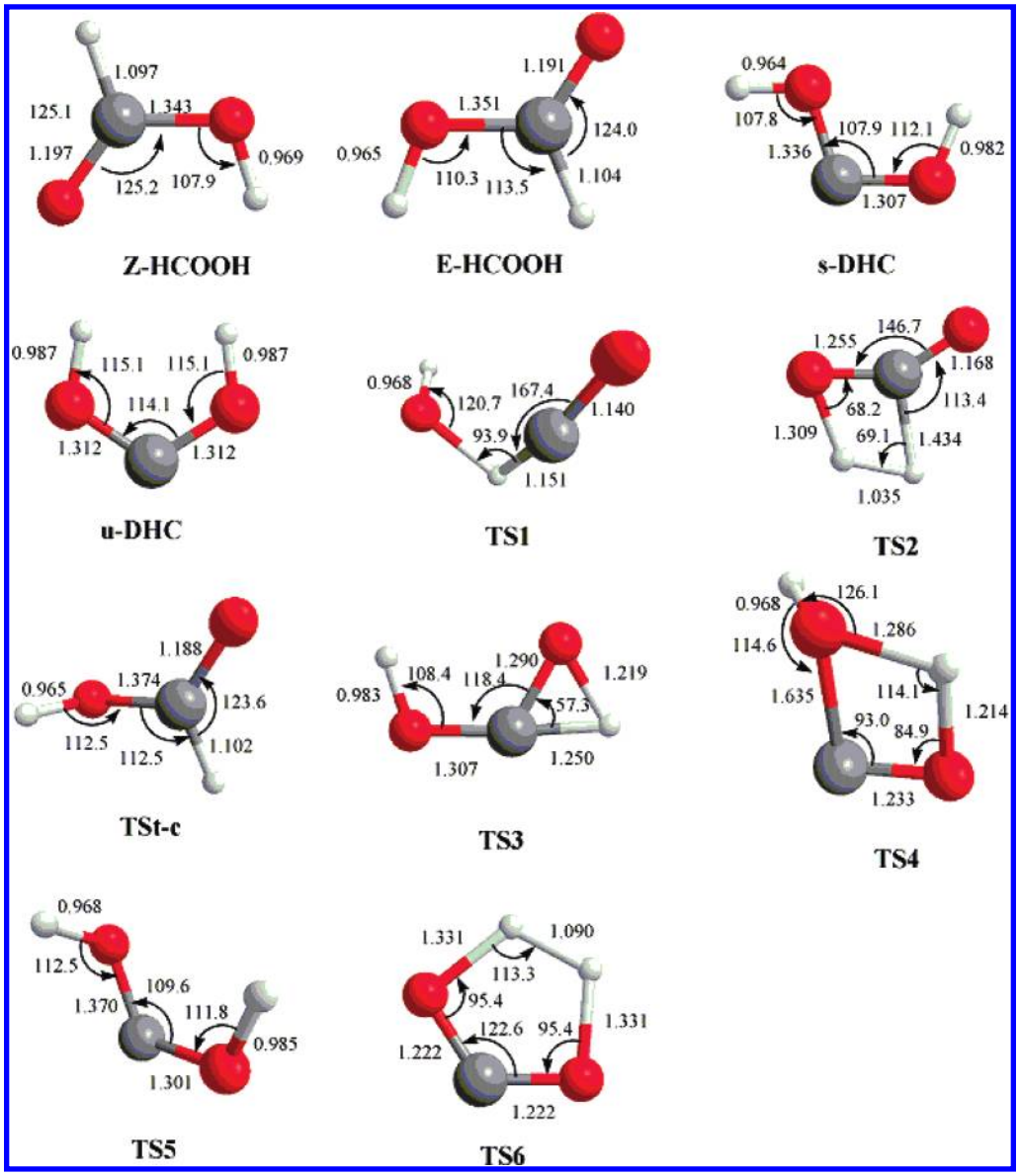

Figure 1. Optimized geometries of the intermediates and transition states of the unimolecular decomposition of formic acid calculated at the B3LYP/6-311+G(3df,2p) level.

interpretations of the data obtained experimentally for both systems. In this work, we report unimolecular decomposition mechanisms for both acids in the gas phase based on detailed potential energy surfaces (PESs) calculated by the high-level G2M(CC1) method.[22] We also provide rate constants for all individual channels mentioned above predicted by means of statistical theory analysis and compare our results with the reported values.

Computational Methods

The optimized geometries of the reactants, intermediates, transition states, and products for the two acid decomposition reactions in the gas phase were calculated at the B3LYP/6-311+G(3df,2p) level.[23−25] The vibrational frequencies were calculated at this level for the characterization of zero-point energy (ZPE) corrections to the stationary points. To obtain more reliable values of energies for PES and rate-constant predictions, we performed a series of single-point energy calculations for each stationary point with the modified GAUSSIAN-2 (G2M) method according to the G2M(CC1) scheme[22] based on the optimized geometries at the B3LYP/6-311+G(3df,2p) level. The G2M(CC1) composite scheme is given as follows:

$$E[\mathrm{G2M(CC1)}] = E_{\mathrm{bas}} + \Delta E(+) + \Delta E(\mathrm{2df}) + \Delta E(\mathrm{CC}) + \Delta + \Delta E(\mathrm{HLC, CC2}) + \mathrm{ZPE}$$

where

$$E_{\mathrm{bas}} = E[\mathrm{PMP4/6\text{-}311G(d,p)}]$$

$$\Delta E(+) = E[\mathrm{PMP4/6\text{-}311+G(d,p)}] - E_{\mathrm{bas}}$$

$$\Delta E(\mathrm{2df}) = E[\mathrm{PMP4/6\text{-}311+G(2df,p)}] - E_{\mathrm{bas}}$$

$$\Delta E(\mathrm{CC}) = E[\mathrm{CCSD(T)/6\text{-}311+G(d,p)}] - E_{\mathrm{bas}}$$

$$\Delta = E[\mathrm{PMP2/6\text{-}311+G(3df,p)}] - E[\mathrm{PMP2/6\text{-}311+G(2df,p)}] - E[\mathrm{PMP2/6\text{-}311+G(d,p)}] + E[\mathrm{PMP2/6\text{-}311G(d,p)}]$$

The higher-level corrections, ΔE(HLC, CC2), are given by $-5.77n_\beta - 0.19n_\alpha$ in millihartrees, where n_α and n_β are the numbers of α and β valence electrons, respectively.

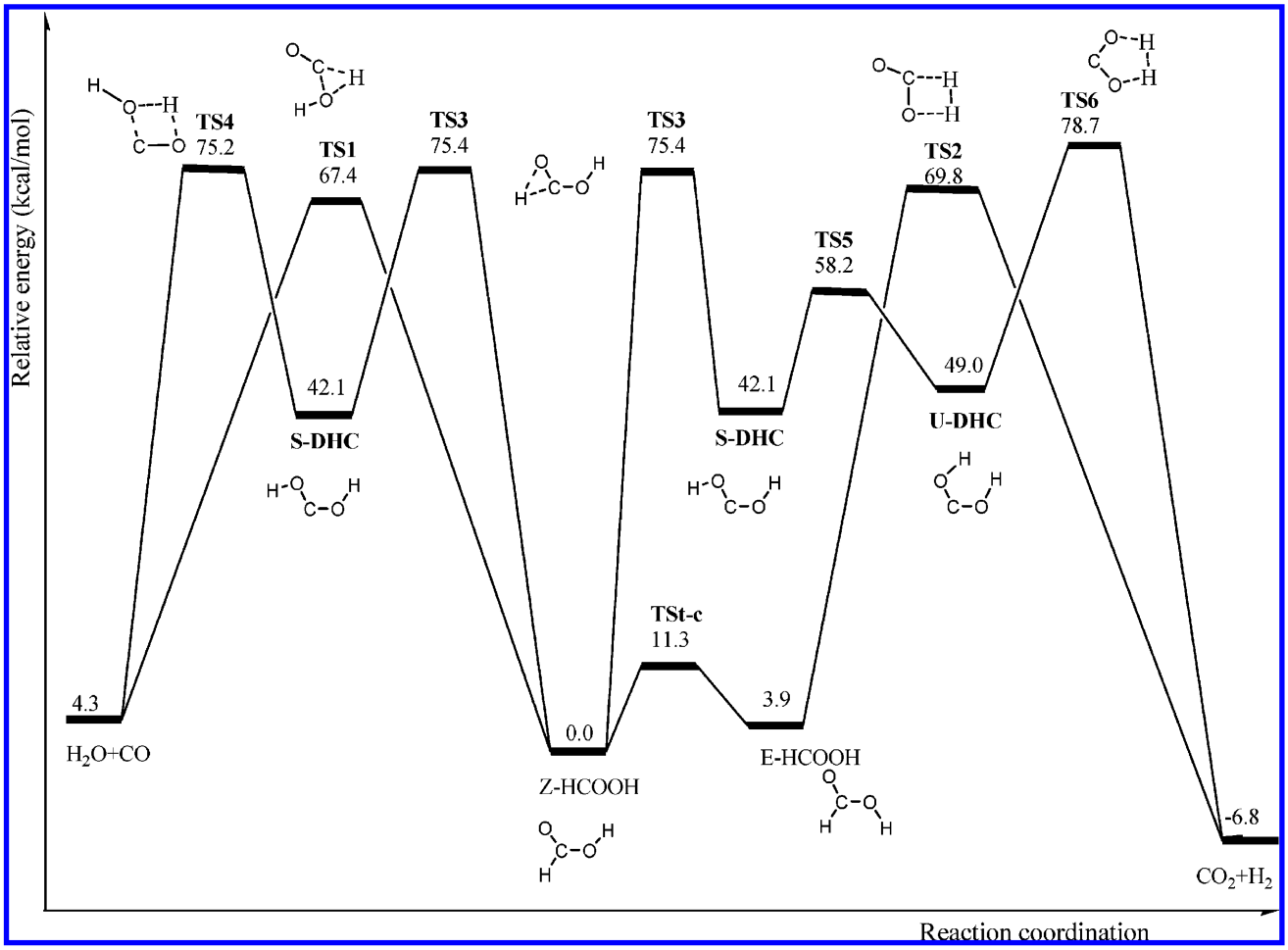

Figure 2. Schematic energy diagram for the decomposition reaction of formic acid calculated at the G2M(CC1)//B3LYP/6-311+G(3df,2p) level, where energy is given in kcal/mol.

The microcanonical Rice−Ramsperger−Kassel−Marcus (RRKM) theory[26−29] was employed to calculate the rate constants for the unimolecular decomposition reactions of formic acid and oxilic acid with the ChemRate code.[30]

Results and Discussion

The calculated geometries and potential energy surfaces of the intermediates and transition states for the unimolecular decomposition of formic acid are summarized in Figures 1 and 2, respectively. The optimized geometries of the rotational isomers of oxalic acid are shown in Figure 3. Figures 4 and 5 present the structures and potential energy surfaces, respectively, of the unimolecular oxalic acid decomposition reaction. In these figures, bond distances are given in angstroms, angles in degrees, and energies in kilocalories per mole. The mechanisms are presented in the following sections in detail. A comparison with previous studies of barrier heights for the decomposition reactions of the two acids in the gas phase is presented in Table 1.

1. Unimolecular Decomposition of Formic Acid. As shown as Figure 1, two configurations of formic acid were identified: the *E* form and the *Z* form. The heat of reaction and barrier height of the *Z*-HCOOH → *E*-HCOOH isomerization are predicted to be 3.9 and 11.3 kcal/mol, in good agreement with the experimental values[31,32] of 3.9 and 10.9 kcal/mol, respectively. The *Z* conformer can also isomerize to dihydroxycarbene (s-DHC) via H transfer from carbon to carboxyl oxygen with a high barrier energy of 75.4 kcal/mol. The dehydration reaction takes place from the *Z* conformer. Two possible channels were found (see Figure 2). First, this process can occur by a concerted step passing over a 67.4 kcal/mol barrier through a three-centered-ring transition state, TS1, to produce H_2O + CO. Second, s-DHC derived from *Z*-HCOOH can decompose to H_2O + CO via a four-centered-ring transition state, TS4. The barrier height of this step is 75.2 kcal/mol. From *E*-HCOOH, the decarboxylation first takes place via the four-centered transition state TS2 to generate CO_2 and H_2 with a barrier height of 65.9 kcal/mol. The products (CO_2 + H_2) also can be formed from a dihydroxycarbene intermediate. As displayed in Figure 2, s-DHC isomerizes to u-DHC by C−O bond rotation and then decomposes to CO_2 and H_2 by passing through the five-centered-ring centered transition state TS6. This stepwise process needs to overcome a high barrier of 78.7 kcal/mol. Our results reveal that the energy required to form dihydroxycarbene (DHC) makes the stepwise channel unfavorable. The calculated barriers for the favored dehydration and decarboxylation are 67.4 and 69.8 kcal/mol, respectively. The results are in good agreement with some of the experimental and theoretical studies listed in Table 1. For the estimation of rate constants, RRKM calculations were performed under the experimental conditions and will be discussed later.

2. Unimolecular Decomposition of Oxalic Acid. *2.1. Isomerization of Oxalic Acid.* First, we studied the rotational isomerization of oxalic acid. According to the internal rotations around the C−O and C−C bonds of oxalic acid, six conformers were identified as shown in Figure 3. In the following text, I-*a* represents isomer *a* (*a* = 1, 2, 3, 4, 5, 6, and 7). It is noticed that I-6 and TS16 do not exist at the B3LYP/6-311+G(3df,2p)

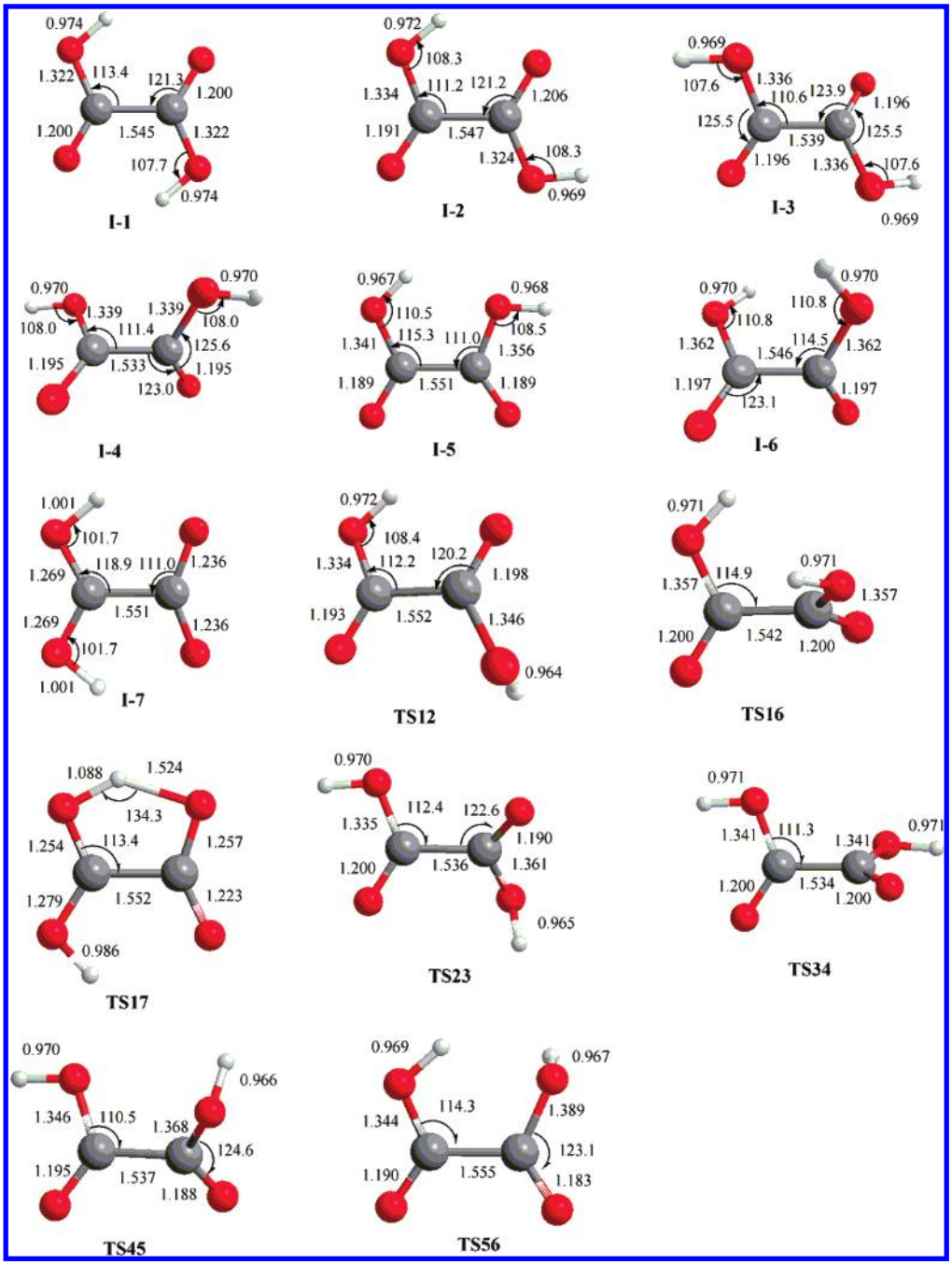

Figure 3. Optimized geometries of the isomers and transition states of the isomerization of oxalic acid calculated at the B3LYP/6-311+G(3df,2p) level.

level, but they can be found at the B3LYP/6-31G(d,p) level. Thus, the energies of I-6 and TS16 were calculated at G2M based on B3LYP/6-31G(d,p)-optimized geometries. I-1, with two intramolecular hydrogen bonds, is the most stable structure among the isomers. The stabilities decrease in the order I-2 > I-3 > I-4 > I-5 > I-6 > I-7. It is interesting that the relative energies of isomers I-1−I-5 vary within 6 kcal/mol, but the relative energies of isomers I-6 and I-7 are much higher at around 13.6 and 22.5 kcal/mol, respectively. Structurally, I-1, I-2, I-5, and I-7 are planar with C_{2h}, C_s, C_s, and C_{2v} symmetries, respectively, but I-3, I-4, and I-6 are nonplanar with C_2 symmetry. The calculated structures of I-3 and I-4 are different from those of Higgins et al.,[20] who predicted I-3 and I-4 to be planar with C_{2h} and C_{2v} symmetry, respectively. The dihedral angles (HO−C−C−OH) of I-3, I-4, and I-6 are 150.1°, 66.5°, and 41.7°, respectively. Earlier theoretical studies based on the Hartree−Fock (HF) level of theory[14,19] gave inconsistent results. HF/6-31G calculations predicted I-3 to be about 0.5 kcal/mol more stable than I-1, whereas HF/6-31G(d,p), MP2/3-21G//HF/3-21G, MP2/6-31G(d)//HF/6-31G, and MP2/4-31G//HF4-31G calculations predicted I-1 to be ∼2, 0.9, ∼2, and 0.8 kcal/mol more stable, respectively, than I-3. In higher-level B3LYP/6-31G(d,p) and MP2/6-31G(d,p) calculations,[16,20] I-1 is the most stable, followed by I-2 and I-3. Our G2M(CC1) results are in good agreement with higher-level B3LYP/6-31G(d,p) and MP2/6-31G(d,p) calculations, as the HF level of theory is unreliable in geometry and energy predictions. Experimentally, I-1 and I-3 were found by an electron diffraction study, and I-1 and I-2 were detected in a matrix isolation study. Our calculated results are more consistent with the matrix IR results.

The pathways for the isomerization of oxalic acid are shown in Scheme 1.

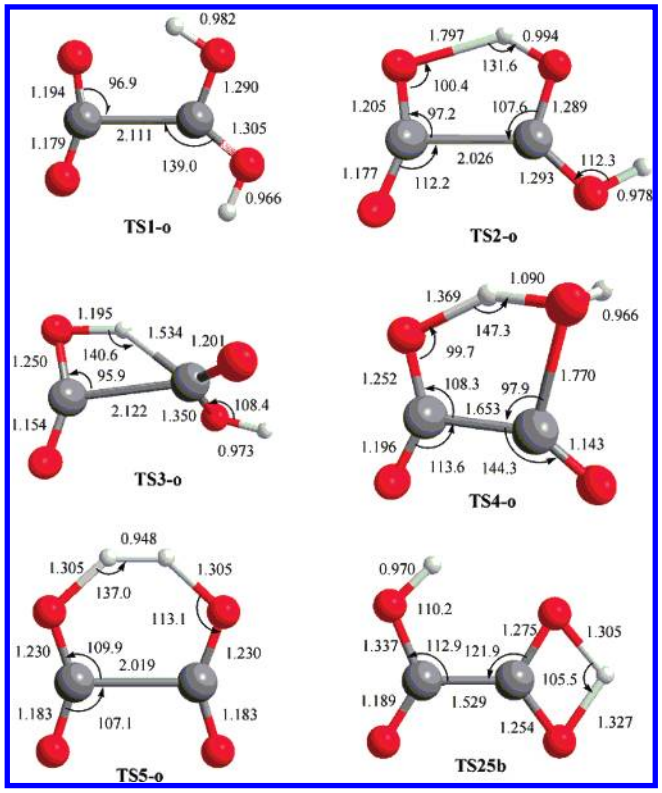

Figure 4. Optimized geometries of the transition states of the unimolecular decomposition of oxalic acid calculated at the B3LYP/6-311+G(3df,2p) level.

The energies given in parentheses are relative to I-1. As illustrated in Scheme 1, I-1 isomerizes to I-2 by rotating the C−O bond via TS12 with a 12.8 kcal/mol barrier. I-1 can also undergo a hydrogen shift to form I-7 with a higher barrier of 21.8 kcal/mol. Then, I-2 can isomerize to I-3 or I-5 via rotation of the C−O bond (TS23) or of the C−C bond with a 10.5 or 5.9 kcal/mol barrier. Subsequent isomerizations can be summarized as follows: I-3 to I-4 by TS34 with a small C−C bond rotational barrier of 0.3 kcal/mol, I-4 to I-5 by TS45 with a C−O bond rotational barrier of 9.9 kcal/mol, I-5 to I-6 by TS56 with a C−O bond rotational barrier of 10.8 kcal/mol, and I-6 to I-1 by TS16 with a small C−C bond rotational barrier of 0.4 kcal/mol. As a result, internal rotations around the C−C bond of oxalic acid occur more easily than internal C−O bond rotations. The low barrier for C−C bond rotation and the steric repulsion between the two hydroxyl groups result in the absence of I-6 at the B3LYP/6-311+G(3df,2p) level of theory.

2.2. Mechanisms for the Decomposition of Oxalic Acid. As depicted by the PES in Figure 5, I-1, I-2, and I-5 are proposed to be the starting reactants in the decomposition of oxalic acid. The possible mechanisms for the decomposition of oxalic acid are as follows:

$$\text{I-1} \rightarrow \text{TS17} \rightarrow \text{I-7} \rightarrow \text{TS1-o} \rightarrow \text{w-DHC} + \text{CO}_2 \quad (3)$$

$$\rightarrow \text{I-2} \rightarrow \text{TS2-o} \rightarrow \text{s-DHC} + \text{CO}_2 \quad (4)$$

$$\rightarrow \text{I-2} \rightarrow \text{TS3-o} \rightarrow \text{HCOOH} + \text{CO}_2 \quad (5)$$

$$\rightarrow \text{I-5} \rightarrow \text{TS4-o} \rightarrow \text{H}_2\text{O} + \text{CO}_2 + \text{CO} \quad (6)$$

$$\rightarrow \text{I-5} \rightarrow \text{TS9} \rightarrow \text{H}_2 + 2\text{CO}_2 \quad (7)$$

First, as suggested above, I-1 can isomerize to I-7 by hydrogen migration via TS17, which is 0.7 kcal/mol lower than I-7 with the ZPE correction but 0.8 kcal/mol higher without the correction. Formation of I-7 is followed by C−C bond cleavage to produce w-DHC and CO_2 via TS1-o. The C···C distance of the broken bond is 2.111 Å. The transition state TS1-o is calculated to be 33.7 kcal/mol above I-1.

The second channel starts from I-2 to decompose to s-DHC and CO_2 simultaneously by a concerted C−C bond cleavage and H-atom migration via TS2-o. The barrier of this process is 36.0 kcal/mol. In TS2-o, the forming O−H bond and the breaking C−C bond are 0.994 and 2.026 Å, respectively. However, the final products of experiments are formic acid (HCOOH) and CO_2. The DHC → formic acid barrier is predicted to be 33.3 kcal/mol (see Figure 2). The apparently high barrier makes this process seem unlikely. We discuss this issue in the following section.

The third path is another possible route to generate HCOOH and CO_2. It can also start from I-2 by passing through the four-membered-ring transition state TS3-o, but with a very high barrier of 70.4 kcal/mol to produce HCOOH and CO_2. The formation of HCOOH and CO_2 via this pathway is thus less competitive because of its high energy barrier.

The fourth decomposition pathway starts from the decomposition of I-5, as shown in Figure 5, to give $H_2O + CO_2 + CO$ via the concerted transition state TS4-o, which is 5.5 and 3.2 kcal/mol higher than TS1-o and TS2-o, respectively. This result is inconsistent with that of Kakumoto et al.,[14] who found this channel to be the main pathway for the decomposition of oxalic acid with a barrier of only 23.7 kcal/mol computed at MP2/3-21G//HF/3-21G or 28.3 kcal/mol at computed MP2/4-31G//HF4-31G. Their prediction is inconsistent with the experiments of Lapidus et al.,[15] who observed HCOOH and CO_2 to be the major products.

The fifth path also starts from I-5 by passing through the concerted transition state TS5-o with a very high barrier of 108.8 kcal/mol to produce H_2 and $2CO_2$. This process can be neglected because of the very high energy barrier.

2.3. Mechanisms for the Isomerization of Dihydroxycarbene. To interpret the fact that HCOOH and CO_2 are the main products of the decomposition of oxalic acid and that they appear in equal amounts, three possible mechanisms for the isomerization of dihydroxycarbene to HCOOH can be proposed: (i) acid-catalyzed isomerization, (ii) bimolecular HOCOH self-reaction, and (iii) quantum-mechanical tunneling.

(i) Acid-Catalyzed Isomerization. To reconcile the oxalic acid decomposition experimental results cited above, Bock and Redington[19] suggested that a bimolecular process using oxalic acid as the catalyst might be the responsible for the formation of HCOOH and CO_2, as shown in Scheme 2. Higgins et al.[20] studied the effect of catalysis by H_2O instead of oxalic acid as an example. The barrier for H_2O-catalyzed conversion calculated at the MP4(SDQ)/6-311++G(d,p)//B3LYP/6-31G(d,p) level was about 31 kcal/mol lower than that for the unimolecular DHC → HCOOH isomerization, suggesting that this mechanism is possible for the analogous oxalic acid-catalyzed DHC isomerization.

(ii) HOCOH Bimolecular Self-Reaction: In this work, we consider another possibility, the bimolecular self-reaction of DHC to produce formic acid, as shown in Scheme 3. As illustrated in path b, six-membered-ring, two-hydrogen-bond complexes, $(\text{w-DHC})_2$ and $(\text{s-DHC})_2$, might be formed first. Then, the two complexes can pass over TSA and TSB by a concerted double-hydrogen-transfer process to produce complexes $(E\text{-HCOOH})_2$ and $(Z\text{-HCOOH})_2$, which can decompose readily to two molecules of *E*-HCOOH and *Z*-HCOOH by breaking two hydrogen bonds. It is noteworthy that we were

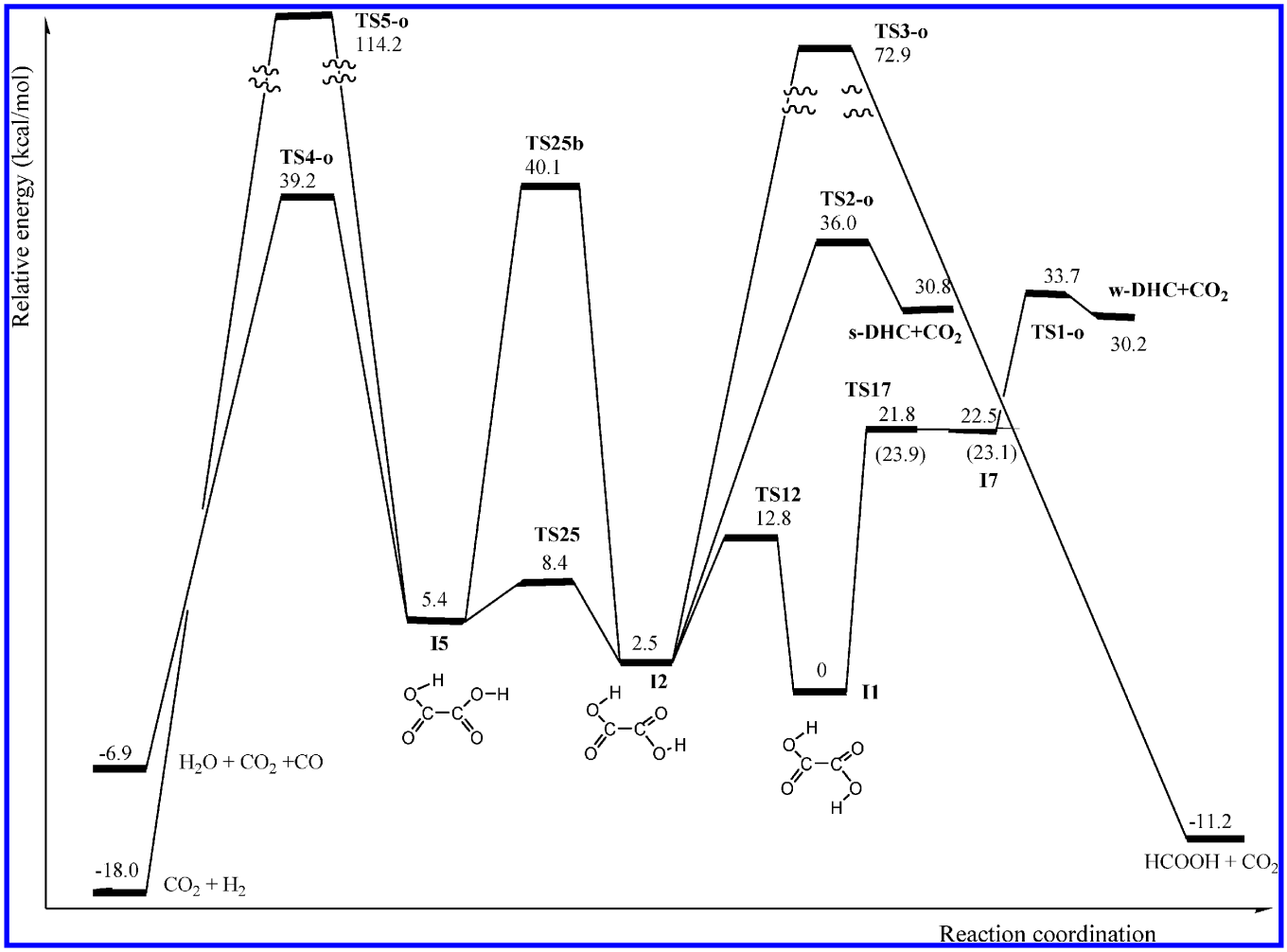

Figure 5. Schematic energy diagram for the decomposition reaction of oxalic acid calculated at the G2M(CC1)//B3LYP/6-311+G(3df,2p) level, where energy is given in kcal/mol. The values in parentheses do not include ZPE corrections.

TABLE 1: Comparison of the Calculated Activation Energies (kcal/mol) of the Unimolecular Decomposition Reactions of Formic Acid and Oxalic Acid with Previous Studies

this work	theoretical	experimental
	Dehydration ($HCOOH \rightarrow H_2O + CO$)	
67.4	67.5 [MP4SDTQ/6-31(d,p)//MP2/6-31G(d,p)][a]	60.5[h]
	70.1 (BAC-MP4 method)[b]	62−65[i]
	63.0 [PMP4/6-311++G(d,p)//UMP2/6-311G(d,p)][c]	
	68 (DZ + PCCSDT-l//DZ + PCCSD)[d]	
	64.6 [B3LYP/6-311++G(3df,3pd)][e]	
	Decarboxylation ($HCOOH \rightarrow CO_2 + H_2$)	
69.8	64.9 (BAC-MP4 method)[b]	65−68[i]
	65.2 [PMP4/6-311++G(d,p)//UMP2/6-311G(d,p)][c]	
	71 (DZ + PCCSDT-l//DZ + PCCSD)[d]	
	66.6 [B3LYP/6-311++G(3df,3pd)][e]	
	Oxalic Acid $\rightarrow HCOOH + CO_2$	
33.7	36.9 [MP4SDTQ/6-311++G(d,p)//B3LYP/6-31G(d,p)][f]	30.0 ± 1.3[j]
	65.5 (MP2/4-31G//HF/4-31G)[g]	
	Oxalic Acid $\rightarrow H_2O + CO_2 + CO$	
39.2	41.9 [MP4SDTQ/6-311++G(d,p)//B3LYP/6-31G(d,p)][f]	
	28.3 (MP2/4-31G//HF/4-31G)[g]	

[a] Reference 9. [b] Reference 12. [c] Reference 6. [d] Reference 7. [e] Reference 10. [f] Reference 20. [g] Reference 14. [h] Reference 2. [i] Reference 3. [j] Reference 15.

not able to locate the $(s\text{-}DHC)_2$ complex. After optimization, the transition from the $(s\text{-}DHC)_2$ complex to the $(Z\text{-}HCOOH)_2$ complex is accompanied by an exothermicity of 87.5 kcal/mol. The relative energies of the $(s\text{-}DHC)_2$ complex and TSA without ZPE corrections [TSA is slightly lower in energy than the $(s\text{-}DHC)_2$ complex with ZPE corrections] are 18.3 and 16.8 kcal/mol, respectively, lower in energy than 2(s-DHC). This process of 2(s-DHC) → 2(*E*-HCOOH) can take place with an overall exothermicity of 75.2 kcal/mol. The optimized structures for the bimolecular isomerization of dihydroxycarbene are presented in Figure S1 (Supporting Information). In principle, it is also possible that two DHC radicals can form a stable intermediate via the formation a strong C═C double bond, producing a tetrahydroxyl ethene that can decompose to HCOOH + H_2O

SCHEME 1

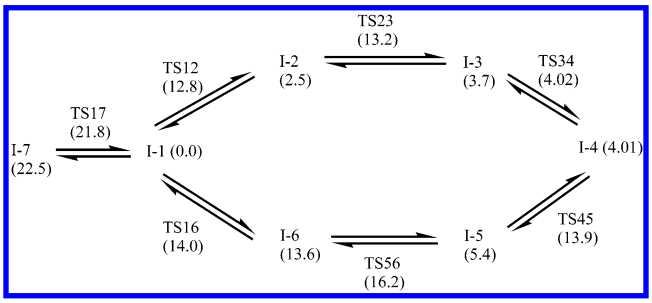

SCHEME 2

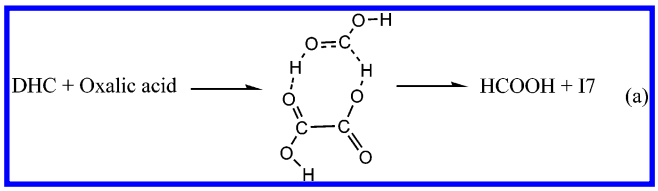

+ CO or $2H_2O$ + 2CO (see path c). The occurrence of this process, however, might affect and fail to account for the experimental observation of the equal yields of HCOOH and CO_2.

(iii) Quantum-Mechanical Tunneling Effect. Although the barrier for DHC → HCOOH conversion shown in Figure 2 is as high as 33 kcal/mol, the effect of quantum-mechanical tunneling for this process might enhance this isomerization rate. Our preliminary calculations carried out at 400 K show that the rate constant of the isomerization reaction is over 30 times greater than that for the oxalic decomposition reaction; the results of kinetic modeling indeed show that the yields of CO_2 and HCOOH are exactly equal at the end of a pyrolysis time under the conditions employed by Lapidus et al.[15] Further study on this and the bimolecularly catalyzed DHC → HCOOH isomerization reaction should be carried out in the future.

3. Rate Constant Calculations

The microcanonical Rice−Ramsperger−Kassel−Marcus (RRKM) theory was used to calculate the rate constants for the unimolecular decomposition reactions of formic acid and oxalic acid. The effects of quantum-mechanical tunneling on the decomposition reactions were considered in these calculations (on the basis of the Eckart model implemented in the ChemRate program). The moments of inertia and vibrational frequencies of the reactants and transition states presented in Table S1 of the Supporting Information were used. The Lennard-Jones (L-J) parameters employed for the formic acid decomposition reaction were as follows: for Ar, σ = 3.75 Å, ϵ/k = 144 K, and for HCOOH, σ = 3.95 Å, ϵ/k = 519 K. The values of the parameters for the oxalic acid system were as follows: for Ar, σ = 4.05 Å, ϵ/k = 162 K, and for $(HCOOH)_2$, σ = 4.56 Å, ϵ/k = 656 K. The formulas used were $\epsilon/k = 0.897T_c$ and $\sigma = 0.785V_c^{1/3}$.[33]

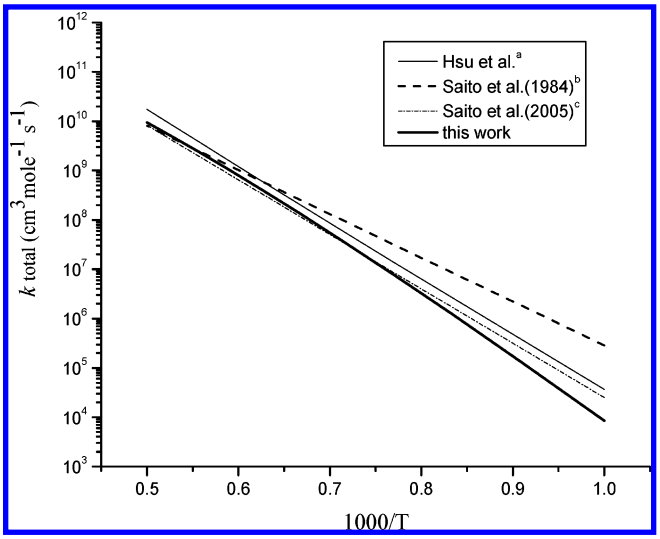

Figure 6. Predicted total rate constants for formic acid decomposition. Data for plots a−c are from refs 3, 4, and 34, respectively.

3.1. Unimolecular Decomposition Reaction of Formic Acid. As mentioned above, the decomposition mechanism of formic acid involves two channels: (1) dehydration and (2) dehydrogenation. The predicted and experimental rate constants (k_{total}) and the branching constants (k_1 and k_2) are compared with available experimental data in Figures 6 and 7, respectively. The calculated Arrhenius expressions for dehydration (k_1) and dehydrogenation (k_2) at the low-pressure and high-pressure limits for the temperature range 500−2000 K can be represented as

$$k_1^0 = 4.05 \times 10^{15} \exp(-52.98 \text{ kcal mol}^{-1}/RT) \text{ cm}^3 \text{ mol}^{-1} \text{ s}^{-1}$$

$$k_2^0 = 1.69 \times 10^{15} \exp(-51.11 \text{ kcal mol}^{-1}/RT) \text{ cm}^3 \text{ mol}^{-1} \text{ s}^{-1}$$

and

$$k_1^\infty = 7.49 \times 10^{14} \exp(-68.71 \text{ kcal mol}^{-1}/RT) \text{ s}^{-1}$$

$$k_2^\infty = 4.46 \times 10^{13} \exp(-68.24 \text{ kcal mol}^{-1}/RT) \text{ s}^{-1}$$

Our low-pressure results are in close agreement with the

SCHEME 3

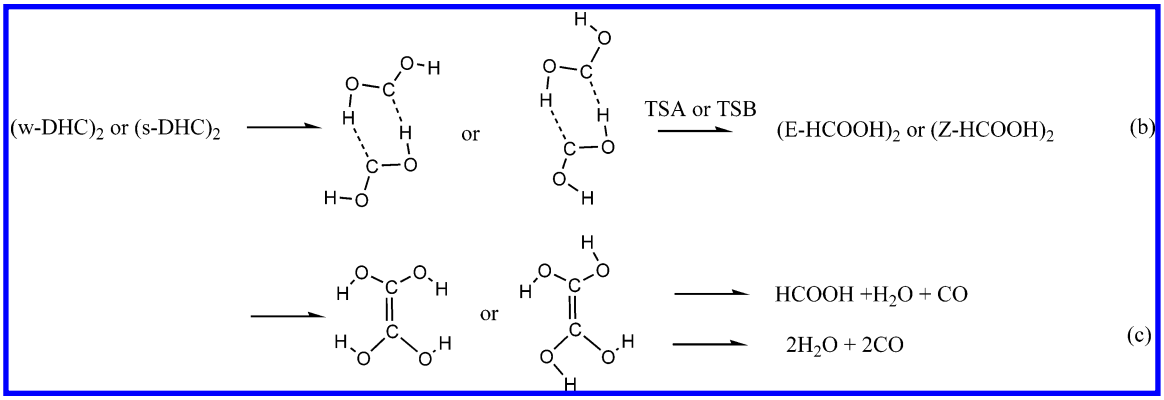

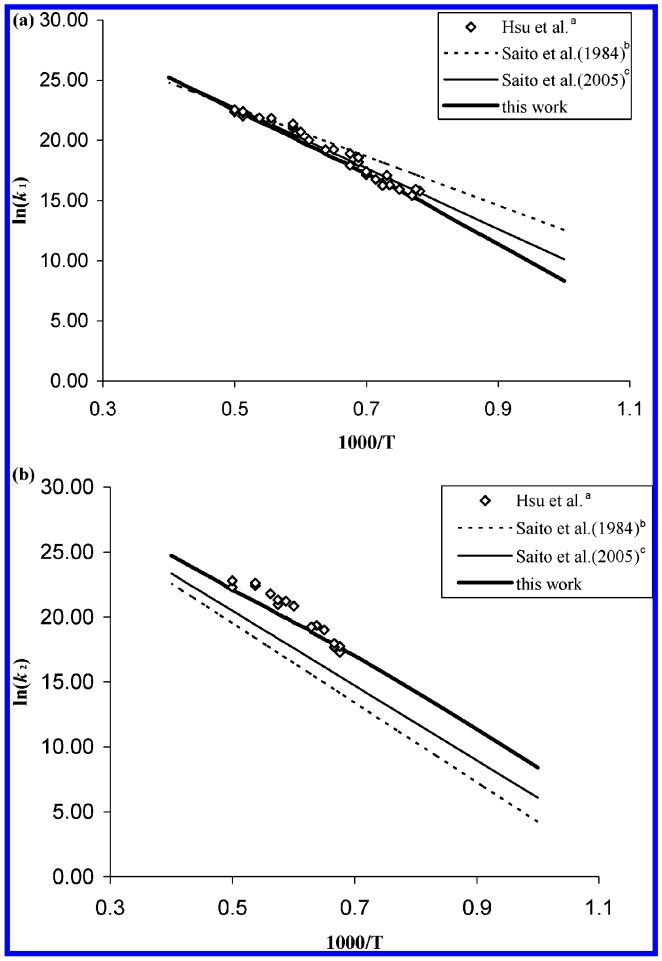

Figure 7. Predicted second-order rate constants in units of $cm^3\ mol^{-1}\ s^{-1}$ for formic acid decomposition: (a) dehydration, k_1; (b) decarboxylation, k_2. Data for plots a−c are from refs 3, 4, and 34, respectively. Ar represents a third body.

experimental data,[3,4,34] particularly those reported by Hsu et al.,[3] over the temperature range studied. In addition, the calculated rate constant for dehydration is $1.94 \times 10^{-7}\ s^{-1}$ at 700 K, which is consistent with the values of 3.25×10^{-7} and $2.03 \times 10^{-7}\ s^{-1}$ reported by Black et al.[2] and Akiya et al.,[35] respectively. The calculated CO/CO_2 ratio is 13.57−13.90 between 1300 and 2000 K, which is in good agreement with the ratio of 10 measured experimentally by Hsu et al.[3]

3.2. Unimolecular Decomposition Reaction of Oxalic Acid. We carried out RRKM calculations for the following major reaction channels based on the PES and mechanism presented in the preceding section:

$$\text{I1} \rightarrow \text{TS17} \rightarrow \text{I7} \rightarrow \text{TS1-o} \rightarrow \text{w-DHC} + CO_2 \quad (3)$$

$$\rightarrow \text{I2} \rightarrow \text{TS2-o} \rightarrow \text{s-DHC} + CO_2 \quad (4)$$

$$\rightarrow \text{I5} \rightarrow \text{TS4-o} \rightarrow H_2O + CO_2 + CO \quad (6)$$

for which the rate constants, k_3, k_4, and k_6, are controlled by the well-defined states TS1-o, TS2-o and TS4-o, respectively. The predicted and experimental values of k_3, k_4, and k_6 are compared in Figure 8. The predicted high-pressure, first-order rate constants for the three decomposition reactions producing w-DHC + CO_2, s-DHC + CO_2, and H_2O + CO_2 + CO in the temperature range 300−2000 K

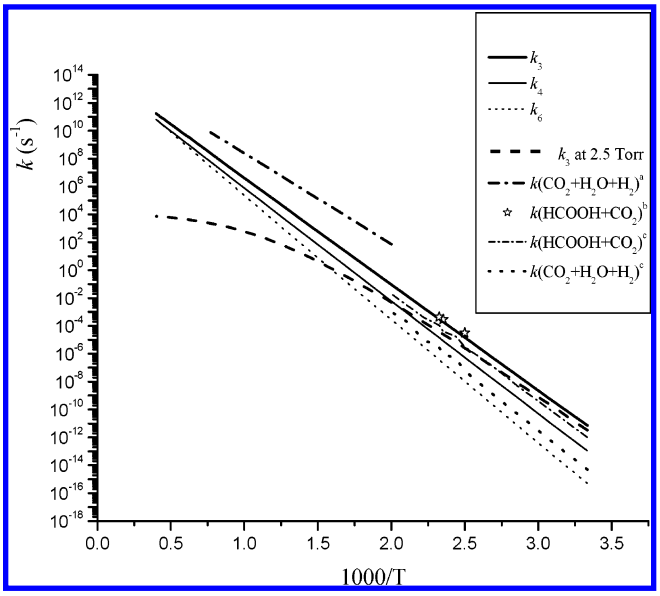

Figure 8. Predicted rate constants for oxalic acid decomposition. Data for plots a−c are from refs 14, 15, and 20, respectively.

can be given by

$$k_3^{\infty} = 1.77 \times 10^{14} \exp(-34.79\ \text{kcal mol}^{-1}/RT)\ s^{-1}$$

$$k_4^{\infty} = 9.85 \times 10^{13} \exp(-36.92\ \text{kcal mol}^{-1}/RT)\ s^{-1}$$

$$k_6^{\infty} = 1.77 \times 10^{14} \exp(-40.50\ \text{kcal mol}^{-1}/RT)\ s^{-1}$$

The rate constant for the formation of HCOOH + CO_2 is $k_3 + k_4$. The expression for $(k_3 + k_4)$ is $2.32 \times 10^{14} \exp(-34.98\ \text{kcal mol}^{-1}/RT)\ s^{-1}$. As shown in Figure 8, the predicted values of k_3 in the experimental temperature range 400−430 K at 2.5 Torr oxalic acid pressure are in excellent agreement with the experimental data reported by Lapidus et al.[15] The predicted values of $(k_3 + k_4)/k_6$, 16.60−3.55 at 1000−2500 K, also agree with the experimental value[18] of >2.6. The calculated results reveal that channel 6 of oxalic acid decomposition becomes more competitive at high temperatures. The predicted rate constants in the low-pressure limit at 300−2000 K can be given by

$$k_3^0 = 1.07 \times 10^{22} T^{-0.00897} \exp(-33.35\ \text{kcal mol}^{-1}/RT)\ cm^3\ mol^{-1}\ s^{-1}$$

$$k_4^0 = 2.22 \times 10^{22} T^{-0.009} \exp(-35.64\ \text{kcal mol}^{-1}/RT)\ cm^3\ mol^{-1}\ s^{-1}$$

$$k_6^0 = 5.56 \times 10^{22} T^{-0.00903} \exp(-38.79\ \text{kcal mol}^{-1}/RT)\ cm^3\ mol^{-1}\ s^{-1}$$

Conclusions

The structures and isomerization and decomposition mechanisms of formic acid and oxalic acid have been studied with the high-level G2M method. Microcanonical RRKM calculations were carried out to evaluate the unimolecular decomposition kinetics. Our results show that dehydration is the main pathway for the decomposition of formic acid. The predicted low-pressure rate constants for unimolecular dehydration and decarboxylation in the gas phase can be given by $k_1^0 = 4.05 \times 10^{15} \exp(-52.98\ \text{kcal mol}^{-1}/RT)\ cm^3\ mol^{-1}\ s^{-1}$ and $k_2^0 = 1.69$

$\times 10^{15}$ exp(−51.11 kcal mol^{-1}/*RT*) cm^3 mol^{-1} s^{-1}, which are in good agreement with the experimental results. The calculated CO/CO_2 ratio, 13.57−13.90, between 1300 and 2000 K, is in good agreement with the experimental value of 10. For the oxalic acid system, similar to other theoretical results, structure I-1 with two intramolecular hydrogen bonds is the most stable structure among the isomers. Two primary decomposition channels producing CO_2 + dehydroxycarbene (DHC) with barriers of 33−36 kcal/mol and $CO_2 + CO + H_2O$ with a barrier of 39 kcal/mol were found. The predicted results can quantitatively explain the observation that CO_2 and HCOOH are the major products in the vapor-phase thermal decomposition of oxalic acid. The predicted high-pressure rate constant for the formation of CO_2 and HCOOH can be represented by $(k_3 + k_4) = 2.32 \times 10^{14}$ exp(−34.98 kcal mol^{-1}/*RT*) s^{-1}. With increasing temperature, the formation of $H_2O + CO_2 + CO$ becomes more competitive.

Acknowledgment. We gratefully acknowledge (1) financial support from the Office of Naval Research under a MURI grant (Prime Award # N00014-04-1-0683 and Subaward # 2794-EU-ONR-0683), (2) the Emerson Center for the use of its resources, and (3) the use of CPUs from National Center for High-performance Computing, Taiwan. M.C.L. acknowledges support from the National Science Council of Taiwan for his distinguished visiting professorship.

Supporting Information Available: Frequencies and moments of inertia I_i of the decomposition reaction of formic acid and oxalic acid calculated at the B3LYP/6-311+G(3df,2p) level and optimized structures of bimolecular isomerization of dihydroxycarbene (Figure S1). This material is available free of charge via the Internet at http://pubs.acs.org.

References and Notes

(1) Chameides, W. L.; Davis, D. D. *Nature* **1983**, *304*, 427.
(2) Black, P. G.; Davis, H. H.; Jackson, G. E. *J. Chem. Soc. B* **1971**, 1923.
(3) Hsu, D. S.; Shaub, W. M.; Blackbum, M.; Lin, M. C. In *The 19th International Symposium on Combustion*; The Combustion Institute: Pittsburgh, PA, 1983; p 89.
(4) Saito, K.; Kakamoto, T.; Kuroda, H.; Torii, S.; Imamura, A. *J. Chem. Phys.* **1984**, *80*, 4989.
(5) Samsonov, Y. N.; Petroy, A. K.; Baklanov, A. V.; Vihzin, V. V. *React. Kinet. Catal. Lett.* **1976**, *5*, 197.
(6) Francisco, J. S. *J. Chem. Phys.* **1992**, *96*, 1167.
(7) Goddard, J. D.; Yamaguchi, Y.; Schaefer, H. F., III. *J. Chem. Phys.* **1992**, *96*, 1158.
(8) Ruelle, P. *J. Am. Chem. Soc.* **1987**, *109*, 1722.
(9) Ruelle, P.; Kesselring, U. W.; Nam-Tran, H. *J. Am. Chem. Soc.* **1986**, *108*, 371.
(10) Wang, B.; Hou, H.; Gu, Y. *J. Phys. Chem. A* **2000**, *104*, 10526.
(11) Corkum, R.; Willis, C.; Back, R. A. *Chem. Phys.* **1977**, *24*, 13.
(12) Melius, C. F.; Bergan, N. E.; Shepherd, J. E. water-catalyzed-theoretical. In *Proceedings of the International Symposium on Combustion*; The Combustion Institute: Pittsburgh, PA, 1990; p 217.
(13) Clack, L. W. *J. Am. Chem. Soc.* **1955**, *77*, 6191.
(14) Kakumoto, T.; Saito, K.; Imamura, A. *J. Phys. Chem.* **1987**, *91*, 2366.
(15) Lapidus, G.; Barton, D.; Yankwich, P. E. *J. Phys. Chem.* **1964**, *68*, 1863.
(16) Nieminen, J.; Rasanen, M.; Murto, J. *J. Phys. Chem.* **1992**, *96*, 5303.
(17) Wobbe, D. E.; Noyes, W. A., Jr. *J. Am. Chem. Soc.* **1926**, *48*, 2856.
(18) Yamamoto, S.; Back, R. A. *J. Phys. Chem.* **1985**, *89*, 622.
(19) Bock, C. W.; Redington, R. L. *J. Chem. Phys.* **1986**, *85*, 5391.
(20) Higgins, J.; Zhou, X.; Liu, R.; Huang, T.-S. *J. Phys. Chem. A* **1997**, *101*, 2702.
(21) Van, Alsenoy, C.; Klimkowski, V. T.; Schafer, L. *J. Mol. Struct. (THEOCHEM)* **1984**, *109*, 321.
(22) Mebel, A. M.; Morokuma, K.; Lin, M. C. *J. Chem. Phys.* **1995**, *103*, 3171.
(23) Becke, A. D. *J. Chem. Phys.* **1992**, *96*, 2155.
(24) Becke, A. D. *J. Chem. Phys.* **1992**, *97*, 9173.
(25) Becke, A. D. *J. Chem. Phys.* **1993**, *98*, 564.
(26) Klippenstein, S. J. *J. Chem. Phys.* **1992**, *96*, 367.
(27) Klippenstein, S. J.; Marcus, R. A. *J. Chem. Phys.* **1987**, *87*, 3410.
(28) Wardlaw, D. M.; Marcus, R. A. *Chem. Phys. Lett.* **1984**, *110*, 230.
(29) Wardlaw, D. M.; Marcus, R. A. *J. Chem. Phys.* **1985**, *83*, 3462.
(30) Mokrushin, W. B., V.; Tsang, W.; Zachariah, M.; Knyazev, V. *ChemRate*, version 1.5.2; National Institute of Standards and Technology: Gaithersburg, MD, 2006.
(31) Bjarnov, E.; Hocking, W. H. *Z. Naturforsch. A* **1978**, *33*, 610.
(32) Miyazawa, T.; Pitzer, K. S. *J. Chem. Phys.* **1959**, *30*, 1076.
(33) Mourits, F. M.; Rummens, F. H. A. *Can. J. Chem.* **1977**, *55*, 3007.
(34) Saito, K.; Shiose, T.; Takahashi, O.; Hidaka, Y.; Aiba, F.; Tabayashi, K. *J. Phys. Chem. A* **2005**, *109*, 5352.
(35) Akiya, N.; Savage, P. E. *AIChE J.* **1998**, *44*, 405.